LATVIAN JOURNAL OF PHYSICS AND TECHNICAL SCIENCES
2013, N 1
DOI: 10.2478/lpts-2013-0004

CHROMOPHORE POLING IN THIN FILMS OF ORGANIC GLASSES. 3. SETUP FOR CORONA TRIODE DISCHARGE

O. Vilitis, E. Titavs, E. Nitiss, M. Rutkis

Institute of Solid State Physics, University of Latvia,
8 Ķengaraga Str., Riga, LV-1063, LATVIA
oskarsvil@gmail.com

The corona discharge is described focusing on the advantages of corona triode techniques for the direct current (DC) positive poling of optical polymers. The proposed experimental setup allows the corona poling of nonlinear optical (NLO) polymers in the modes of DC constant current (the lowest 1nA) and of the fixed corona-grid voltage, making it possible to carry out the corona-onset poling at elevated temperature (COPET) up to 200 ^{o}C. The setup also provides a wide range of the corona discharge voltage (3 kV – 15 kV), variable reciprocal distance of electrodes as well as the possibility to choose from different types of the corona electrode (needle, multi-needle, wire, etc.). By keeping the corona-to-grid voltage constant, a stable corona discharge at electrode is attained. The grid voltage can be varied in the range from 0 to 3kV. The corona poling area on the sample surface is pre-defined by placing ring spacers above it. The setup is completely computerized, allowing both control and monitoring of the corona discharge, which promotes research into the process of charging NLO polymer samples and selection of the optimal poling mode. Using the voltage-current characteristics and the second-harmonic measurements of a poled polymer we also demonstrate the influence of the setup parameters on the efficiency of poling the thin film NLO polymers.

Key words: *corona discharge, corona triode poling, poled polymer*.

1. INTRODUCTION

Second-order nonlinear optical (NLO) polymer materials are highly attractive for applications in electro-optic (EO) devices due to their large optical nonlinearity, low cost and ease of processing. NLO polymer films could be widely used in optic and electronic applications, e.g. second harmonic generation (SHG), EO phase modulation, parametric amplification for optical switching, etc. For the second-order nonlinearities a non-centrisymmetrical alignment of NLO chromophores is needed, which is achieved during a poling process.

For poling NLO polymer films in the external electric field several techniques exist (e.g. [1, 2]). One of them is poling with corona discharge. Despite the outstanding corona poling experiments in this area, most of the research works were carried out applying rather a primitive and poorly controlled point-to-plane or wire-to-plane versions of the corona discharge method (see, e.g. [3]).

In practice, charging with simple means (as applied in two-electrode systems) does not provide the efficiency required for NLO polymer poling [2, 4]; therefore, two-electrode chargers were gradually replaced by the three-electrode ones (also called corona triodes). For better control of the poling process, a metal grid is introduced into the corona triode between the sample and a corona electrode. Recently, the corona triode has been improved by controlling the grid voltage to provide the poling under constant current [3]. According to this method, the sample's potential as function of time is evaluated from the grid voltage. The method allows monitoring the voltage buildup on the sample's surface during the poling process, when information is needed for evaluation of the dipolar orientation.

2. CORONA TRIODE SETUP FOR POLING THE THIN FILMS OF ORGANIC NLO POLYMER

The corona triode setup (charger) for NLO polymer poling is schematically shown in Fig. 1. The charger consists of three major components.

The base component is a planar conductive opposite electrode (thin ITO or Au film) on a ~ 1 mm thick glass substrate. The polymer films (~1 μm thick) are spin-coated directly on the opposite electrode. During the procedure of poling the bare surface of glass substrate is pressed tightly to the polished area of the heating platform of a copper block, the temperature of which is measured with a thermo-sensor located near the glass substrate and controlled by the voltage drop on heating resistors. A cooling fan is used to increase the rate of cooling the copper block.

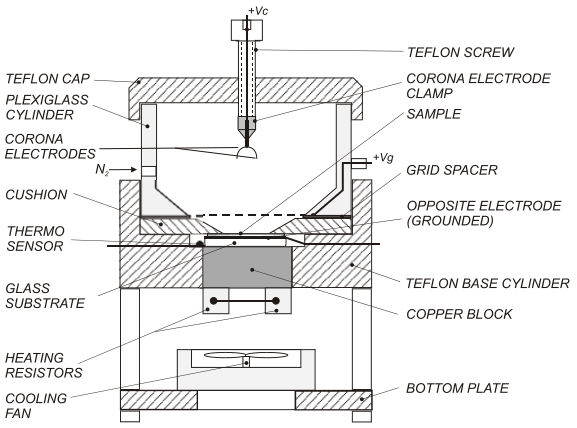

Fig. 1. Schematic setup of the corona triode unit for NLO polymer poling.

The second component is a crosswise-located stainless steel grid with the optical transparency of ~ 0.5. The sample-to-grid distance can be varied with cushion rings of different thickness. In addition ring, a Teflon mask (thickness ~ 20 μm) or a grounded metal mask can also be integrated to bound the poling area of the sample.

The third main component is a corona electrode (see Fig. 1). In our case the corona electrode is formed of a 20 μm tungsten wire arc with two scarf endings.

The corona electrode holder has a clamp which allows replacing or changing easily different electrode modifications. The holder is centred in a Teflon cap with a screw to allow varying the distance of wire above the grid (1–5 cm). The Teflon cap together with both the cylinders (Plexiglas and Teflon base) separates the corona discharge space from the external environment. The Plexiglas cylinder is equipped with a gas opening for operation in nitrogen or another gaseous medium.

The block diagram of the corona triode unit for NLO polymer poling is shown in Fig. 2.

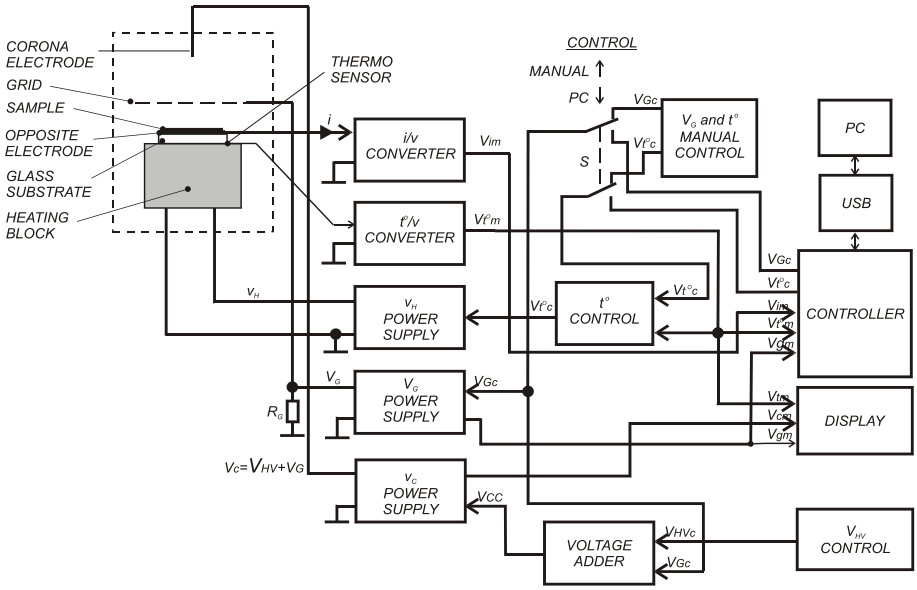

Fig. 2. Block diagram of the corona triode unit for NLO polymer poling.

Here the corona grid is powered by a high-voltage (*Vg*) power supply (HVPS, WME S3-3P-L12 model), which operates in the range 0–3 kV. The corona electrode is powered by a high-voltage (*Vc*) HVPS (UltraVolt 20A12-P4-C model) operating in the range 3–15 kV. The corona electrode working mode is held independent of grid potential v_G by keeping corona electrode voltage v_C and grid voltage difference constant: $v_C - v_G = 5$ kV. As can be seen in the block diagram of Fig. 2, the output voltage v_C of v_C *POWER SUPPLY* is determined by the control voltage v_{CC} at the output of *VOLTAGE ADDER* block. One input of this block is connected to v_{HVC} control voltage from v_{HV} *CONTROL* block, and the other input to the grid voltage control signal v_{GC}. Control voltage $v_{CC} = v_{GC} + v_{HVC}$ defines the corona electrode supply voltage $v_C = V_{HV} + v_G$ at the output of v_C *POWER SUPPLY* block, where V_{HV} is a chosen constant (the difference between corona electrode voltage v_C and grid voltage v_G). For example, at $V_{HV} = 5$ kV = *const* and $v_G = 3$ kV the corona electrode voltage $v_C = 5$ kV + 3 kV = 8 kV. The grid voltage control signal v_{GC} can be routed to v_G *POWER SUPPLY* and *VOLTAGE ADDER* blocks either from PC-programmed grid control (through *USB* and *CONTROLLER* blocks), or from an autonomous v_{GC} source (block v_G and t^o *MANUAL CONTROL*), depending on the state of switch *S* (Fig. 2).

After applying high voltage to the corona electrodes, the ions generated in the corona region near the electrode follow the field lines to the region of lower potential – i.e. grid. A large amount of these ions will be attracted to the grid, causing appearance of a grid current (~ 70% of the total corona current) [3]. The remaining ions will bypass it and reach the sample surface. It is important to note that the grid current can cause noticeable charging of the exit capacitor of grid power supply – above the setup voltage, because the rectifier of the supply is blocking up the leak of grid current. To prevent this, the grid HVPS output is loaded by the grid current leakage resistor R_G (Fig. 2). By controlling the grid voltage $v_G(t)$ the sample charging current I_0 could be kept constant to determine the sample surface potential $v_S(t)$. This effect is obtained by a current-to-voltage converter and a proportional integral controller (Fig. 1). Wherewith, it is possible to determine the sample potential during the charging process by measuring $v_G(t)$. The sample surface potential is a function of time at constant charging current I_0 and is determined by the equation [3]:

$$v_S(t) = v_G(t) - V_{GAP}, \tag{1}$$

where V_{GAP} – the difference (constant at current I_0 being constant during the charging process) between the grid and the sample surface potentials.

Before starting the sample charging, V_{GAP} is determined from a charging system's i–v_G characteristic, using the bare opposite electrode, when $v_S(t) = 0$ and $v_G = V_{GAP} = V_G$. Therefore, if the experimental conditions are equal, $i = I_0 = const$ and the V_{GAP} as well as $v_G(t)$ values are determined, it is possible to control the $v_S(t)$ changes during a sample poling process.

The poling current I_0 being constant, it is possible to describe three partial currents [4]:

$$I_0 = i_C(t) + i_{CON}(t) + i_P(t), \tag{2}$$

where $i_C(t) = Cdv_C(t)/dt$ is the capacitive component of constant current;
C is the sample capacitance, $C = \varepsilon A/L$;
A is the sample area;
ε is the sample dielectric constant;
L is the sample thickness;
$i_{CON}(t)$ is the conductive component of constant current;
$i_P(t) = AdP(t)/dt$ is the electric polarization component of constant current;
P is the sample electric polarization.

At the beginning of poling the capacitive component $i_C(t)$ is prevailing; however, it is decreasing fast as the capacitor (or the surface of sample with capacity C) is charging.

The electric polarization component $i_P(t)$ is determined by polarization potential $e_P(t)$, which is opposite to the sample surface potential. The polarization potential is gradually increasing while reaching its saturation when the sample is being poled; therefore, it could be assumed that equivalent resistance $r_P(t)$ is gradually growing as current $i_P(t)$ is decreasing. As a result, voltage $v_P(t)$ in the sample poling process is inclining towards its maximum value, while the current component $i_p(t)$ is tending to zero. Wherewith, as $i_c(t) \to 0$ and $i_p(t) \to 0$ at a poling

process' finish state, the sample surface poling potential $V_s(t)$ is determined by the third component $i_{CON}(t)$ of constant current I_0 characterized by the sample active resistance $V_S = I_0 r_{CON}$. If $r_{CON} \to \infty$, then $V_S \to V_G$; therefore, the sample surface voltage V_S cannot exceed the grid voltage V_G.

In the case when the DC component of poling current $I = I_0$ is to be kept constant, the grid voltage is adjusted continuously through a feedback circuit at the output of v_G *POWER SUPPLY* block (see Fig. 2). The poling current *i* from the opposite electrode is flowing to the ground through a small input resistance of the *i/v* (current-to-voltage) *CONVERTER*. A commercially available operational amplifier LMC6082 is used at the input of converter (designed for measuring low current and featuring the ultra-low input bias current (10 fA) and low offset voltage drift (1.0 nV/^{o}C)). The converter device is converting the poling current *i* (to the lowest of 1 nA) into voltage v_{im}, which is continuously registered by a PC through *CONTROLLER* and *USB* blocks. According to the measured v_{im} and depending on the chosen constant current I_0, the PC program determines the control voltage v_{GC} which is routed to the control input of v_G *POWER SUPPLY* block through the feedback circuit *USB-CONTROLLER* and switch *S*. By this, it is achieved that current $I = I_0$ flowing through the sample is kept constant.

Procedure of the kind is used for the sample heating feedback circuit, which is implemented in a similar way: PC program controls the temperature according to the measured sample temperature and depending on the temperature regime chosen for the heating. The *THERMO SENSOR* (in our case a copper-alumel thermocouple) is connected to the input of t^o/v (temperature-to-voltage) *CONVERTER*. The output converter voltage $v_{t^o m}$ is continuously registered in PC through *CONTROLLER* and *USB* blocks and fed to one of the inputs of the temperature control block t^o *CONTROL*. According to the measured $v_{t^o m}$ and depending on the chosen temperature regime, the PC program determines the control voltage $v_{t^o c}$ which is routed to the other input of t^o *CONTROL* block through the feedback circuit *USB-CONTROLLER* and switch *S*. Output voltage $v_{t^o c}$ of the temperature controller controls the v_H *POWER SUPPLY* block. In turn, the output voltage of power supply block feeds the heating elements of the sample's *HEATING BLOCK*. Switch *S* allows commanding of t^o *CONTROL* block to be swapped from the PC programming to the manual control (realized by autonomous V_G and t^o *MANUAL CONTROL* block).

Additionally, the developed PC program allows simultaneous and continuous monitoring of poling current, grid voltage and real-time temperature, as well as simultaneous display of the correlation between parameters in the form of characteristics. If the corona discharge setup is used autonomously (without connection to PC), the control of the aforementioned parameters of the poling mode is to be done using the autonomous digital *DISPLAY* block (see Fig. 2).

3. INFLUENCE OF SETUP PARAMETERS ON THE CORONA POLING EFFICIENCY

The poling efficiency depends on multiple parameters (see e.g. [5]). To optimize them, a reproducible corona poling process was to be developed. We have therefore tried to optimize this process by analyzing the *I – V* characteristics of the

system and evaluating the efficiency of poling the NLO polymer samples. The optimization has been performed in several steps.

First, for good reproducibility we had to exclude the uncertainties of surface charging caused by variations in the ionic flux from the corona electrode. This is mainly influenced by two parameters – the ambient gas composition and the corona-grid voltage difference. To ensure that the temperature and humidity changes have insignificant effect on the discharge process, the air in the corona chamber was substituted by nitrogen. This also has an effect of practically cutting out the generation of ozone in the chamber. As known, during the corona discharge in air there arises a large amount of ozone, which is highly active and, in some cases, can react with NLO active chromophores in the polymer.

To ensure that the experiment is repeatable, it is important to provide a stable and fixed ion flux to the sample. If V_g is increased and V_c is kept constant, the sample current saturates as shown in Fig. 3. This is due to a decrease in the voltage drop between the corona electrodes and the grid with increasing V_g. In order to provide near-ohmic relation in the gap it is suggested keeping the corona electrode-grid voltage constant. As seen in Fig. 3, this parameter is kept constant, and the sample current is almost linearly proportional to V_g.

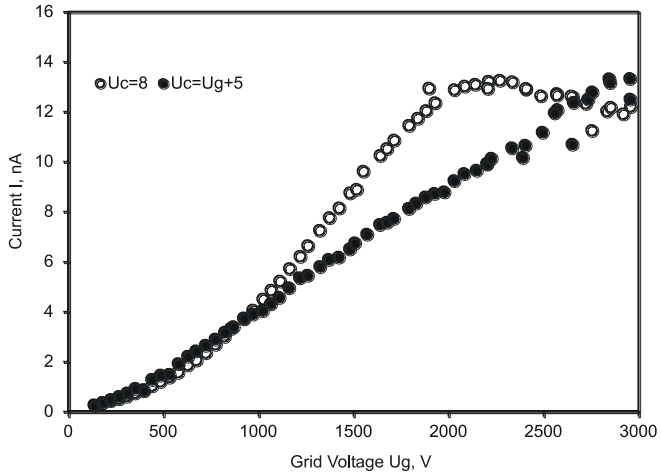

Fig. 3. ITO electrode to grid *I-V* characteristics at constant corona electrode voltage and constant corona electrode-grid voltage difference.

One of the important parameters for a poling procedure is the rate of charging the sample surface, which should be proportional to the ion flux density; this latter, in turn, is proportional to the sample current. This current can be controlled not only by altering V_g, but also by varying the sample-to-grid distance. In our case this can be achieved by placing Teflon rings above the sample. As could be seen in Fig. 4, increasing the sample-to-grid distance reduces the current between the bottom electrode (ITO layer) and the grid. This occurs due to increase in the respective gap resistance.

In Fig. 5, the grid voltage and temperatures are shown as functions of time during a constant current poling (the constant is set to 5 nA). As expected, at the beginning the grid voltage is growing while the sample surface is charged; therefore, charging is the dominant process for 30 s of the poling. Afterwards, owing to

increase in the sample conductance caused by increasing temperature, the grid voltage decreases. Finally, when the thin film surface charging has been finished and the sample temperature stabilized at the poling temperature, the dominant process that determines the sample and, therefore, the grid voltage is that of variation in the polarization potential of the thin film. The poling procedure can be stopped when the grid voltage value stabilizes. In the case shown in Fig. 5 the time after which the poling procedure can be stopped is ~ 240 s.

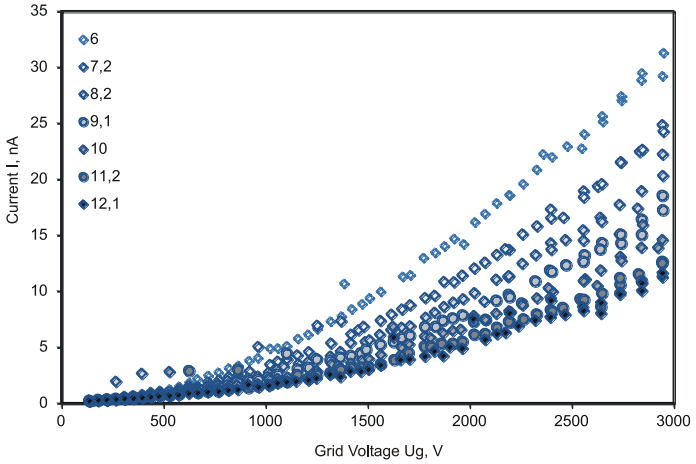

Fig. 4. Measured sample current as a function of the grid voltage at different sample-to-grid distances.

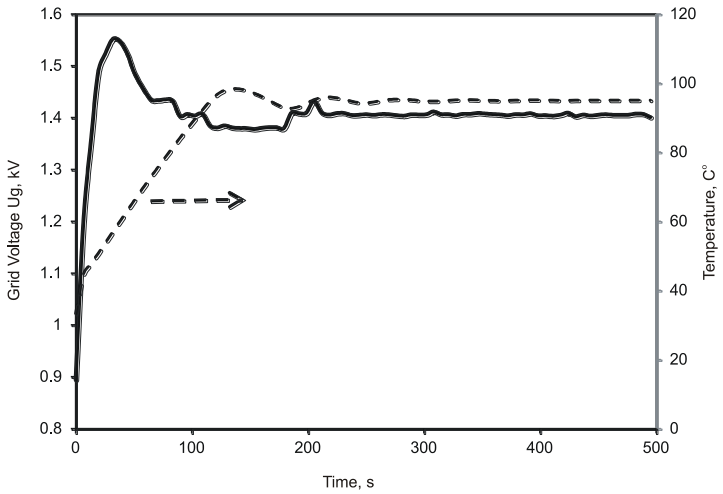

Fig. 5. Grid voltage and temperature as functions of time during constant current poling.

Further investigations concern enhancing the NLO corona poling efficiency, which is determined in terms of effective NLO coefficient – the ratio between the second harmonic generation (SHG) of poled sample and the quartz SH signal maxima. The optimization includes finding the optimal grid-to-sample distance, grid voltage, and spacer shape.

As shown in [5], the poling method using a corona discharge can change the polymer film's morphology, which usually results in formation of pores. These

pores, however, reduce the total observable nonlinearity by scattering of light. In [5] a short pre-heating procedure before the poling is reported to prevent damage of the film. The pre-heating has to be done rather fast (in 3–5 min) to avoid formation of centro-symmetric crystals [6].

As can be seen from Fig. 6, the grid-to-sample distance has no significant impact on the NLO polymer poling efficiency. This means that the sample is being charged to voltage V_s regardless of the intensity of ion flux. Therefore, by increasing the mentioned distance and thus reducing the energy of the ions that reach the sample surface we should reduce the possibility for inhomogeneities to arise and maintain the optimal quality of the film after poling. Also, to maximize the effective NLO coefficient (d_{eff}) the poling fields should be as strong as possible. In Fig. 7 we can see that at increasing grid voltage V_g and thus the poling field, the effective NLO coefficient d_{eff} also increases until saturates at higher grid voltages.

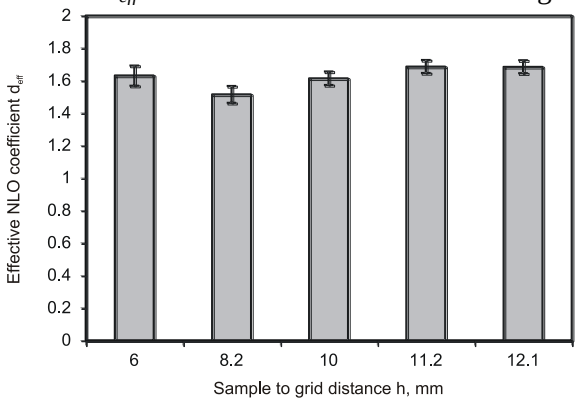

Fig. 6. Effective NLO coefficients for different sample-to-grid distances.

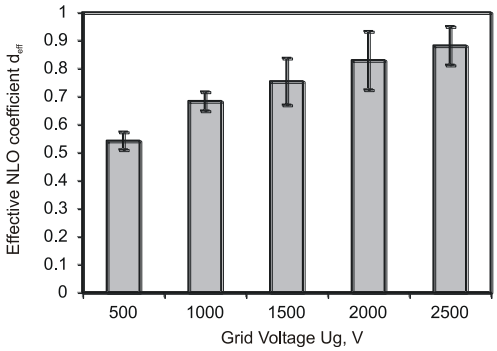

Fig. 7. Effective NLO coefficients for different corona-grid voltages.

In order to complete optimization of the poling setup it was interesting to estimate the influence of spacer shape on the poling efficiency. Our primary assumption was that a spacer with a cone-shaped hole in the middle would act as a lens for the ion flux. Figure 8 shows that effective NLO coefficient d_{eff} is independent of the spacer shape. Again, it should be referred to the sample being charged to voltage V_s regardless of the charging rate. Even if the sample is charged faster when using a conical spacer, the sample poling voltage V_s cannot exceed the grid voltage V_g. In other words, such a spacer defines the rate of capacitor charging,

while effective voltage drop V_s after the charging is defined by the sample and the gap resistance ratio.

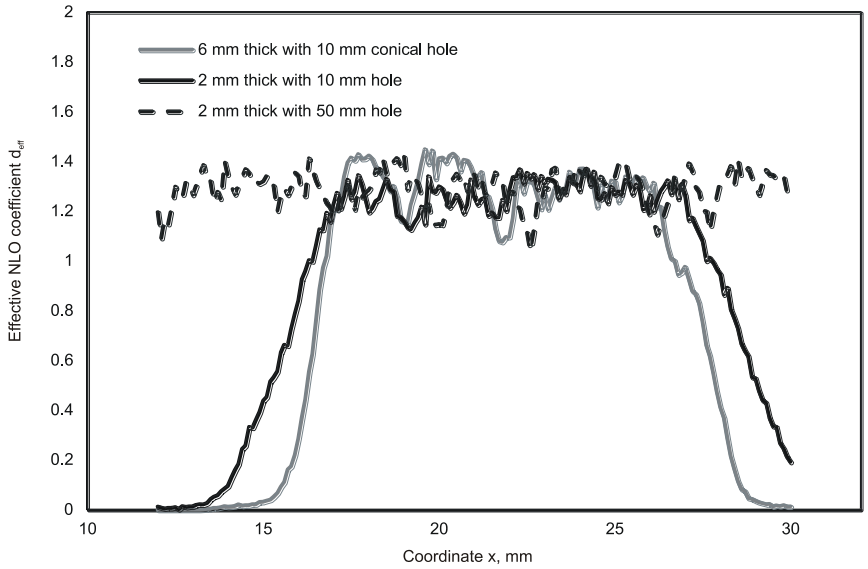

Fig. 8. Effective NLO coefficients for differently shaped spacers.

4. CONCLUSIONS

We have demonstrated and profoundly described the experimental corona triode setup for NLO polymer poling. The corona triode created by us can operate in both constant current and constant voltage modes. We have also performed optimization of the corona poling parameters for a good reproducibility and the maximum NLO poling efficiency. The first steps of this optimization included obtaining the repeatable corona discharge conditions. The influence of ambient temperature and humidity in the corona chamber was eliminated by substituting air by nitrogen. The keeping of the corona electrode-grid voltage constant has allowed us to ensure similar corona discharge conditions independently of the grid voltage. Moreover, in such a way also a near-ohmic relation between the grid voltage and the sample current is provided.

The efficiency of the process can be seriously affected by changes in the surface morphology of a poled thin film. To avoid appearance of surface inhomogeneities it is suggested using the poling procedure which includes preheating the sample. Moreover, it was found advisable to increase the sample-to-grid distance thus reducing the probability of surface damage. At same time, we have demonstrated that this distance does not affect the NLO polymer poling efficiency since the sample surface is charged to a value proportional to the grid voltage regardless of the mentioned parameter.

ACKNOWLEDGEMENTS

This work has been supported by ERDF project (agreement No. 2010/0308/2DP/2.1.1.1.0/10/APIA/VIAA/051) and by the European Social Fund within the project "Support for Doctoral Studies at the University of Latvia".

REFERENCES

1. Vilitis, O., Fonavs, E., & Rutkis, M. (2011). Chromophore poling in thin films of organic glasses. Overview of corona discharge application. *Latv. J. Phys. Tech. Sci., 48* (6), 53–65.
2. Vilitis, O., Muzikante, I., Rutkis, M.,&. Vembris A. (2012). Chromophore poling in thin films of organic glasses. 2. Two-electrode corona discharge setup. *J. Phys. Techn. Sci., 49* (2), 62–70.
3. Dao, P.T., Williams, D.J., McKenna, W.P., & Goppert-Baraducci, K. (1993). Constant current corona charging as a technique for poling organic nonlinear optical thin films and the effect of ambient gas. *J. Appl. Phys., 73* (5), 2043–2050.
4. Giacometti, J.A., Fedosov, S., & Costa, M.M. (1999). Corona charging of polymers: Recent advances on constant current charging. *Brazilian J. Physics, 29* (2), 269–279.
5. Lee, S.S., Garner, S.M., Chuyanov, V., Zhang, H, Steier, W.H., Wang, F., Dalton, L.R., Udupa, A.H., & Fetterman, H.R. (2000). Optical intensity modulator based on a novel electrooptic polymer incorporating a high $\mu\beta$ chromophore. *IEEE J. Quantum Electronics, 36* (5), 527–532.
6. Vembris, A., Rutkis, M., & Laizane, E. (2008). Influence of corona poling procedures on linear and non-linear optical properties of polymer materials containing indandione derivatives as cromophores. *SPIE Proceedings, Organic optoelectronics and photonics III*, 6999(1).

HROMOFORU POLARIZĒŠANA PLĀNĀS ORGANISKO STIKLU KĀRTIŅĀS 3. KORONAS IZLĀDES TRIODES IERĪCE

O. Vilitis, E. Titavs, E. Nitiss, M. Rutkis

K o p s a v i l k u m s

Darba ievadā īsumā aprakstīta koronas izlāde, izceļot koronas triodes theniskās metodes lietošanas priekšrocības optisko polimeru polarizēšanā ar pozitīvās koronas līdzstrāvu. Rakstā apskatīta eksperimentāla koronas polēšanas ierīce, kas sniedz iespēju polarizēt nelineāros optiskos (NLO) polimērus pie konstantas strāvas (līdz pat 1 nA) un fiksēta koronas elektroda-tīkliņa sprieguma, ļaujot veikt polēšanu paaugstinātās temperatūrās līdz 200 ^{o}C. Ierīcē paredzētas plašas koronas izlādes sprieguma izvēles robežas (3–15 kV), iespējas mainīt elektrodu savstarpējo izvietojumu un izvēlēties dažādus koronas elektrodu veidus (adatu, vairākas adatas, stiepli). Ir iespējams nodrošināt pastāvīgu koronas elektroda darba režīmu, saglabājot konstantu spriegumu starp koronas elektrodu un tīkliņu pie tīkliņa sprieguma izmainīšanas iespējām robežās no 0–3 kV. Parauga virsmas polarizēšanas laukumu var mainīt ar gredzenveida starplikām, ko novieto virs parauga virsmas. Ierīce ir pilnībā datorizēta, kas ļauj sekot koronas izlādes gaitai, to vadīt un reģistrēt rezultātus. Tas savukārt uzlabo NLO polimēru paraugu uzlādēšanas procesu pētījumu kvalitāti un ļauj veiksmīgāk noteikt optimālāko polarizēšanas režīmu. Izmantojot strāvas–sprieguma raksturlīknes un polarizēto polimēru otrās harmonikas mērījumus, var arī uzskatāmi parādīt, kā polarizēšanas ierīces un tās darba režīma parametri ietekmē polarizēto plāno kārtiņu NLO efektivitāti.

28.12.2012